Electronic Supporting Information (ESI):

Slow Magnetic Relaxation in a {$EuCu_5$} Metallacrown

Jin Wang,[a] Ze-Yu Ruan,[a] Quan-Wen Li,[a] Yan-Cong Chen,[a] Guo-Zhang Huang,[a] Jun-Liang Liu,[a*] Daniel Reta,[b] Nicholas F. Chilton,[b*] Zhen-Xing Wang[c] and Ming-Liang Tong[a*]

[a] Key Laboratory of Bioinorganic and Synthetic Chemistry of Ministry of Education, School of Chemistry, Sun Yat-Sen University, Guangzhou 510275 (P. R. China)

[b] School of Chemistry, The University of Manchester, Oxford Road, Manchester M13 9PL (UK)

[c] Wuhan National High Magnetic Center, Huazhong University of Science and Technology, Wuhan 430074 (P. R. China)

Table of Contents

S1. Crystal Data and Structures

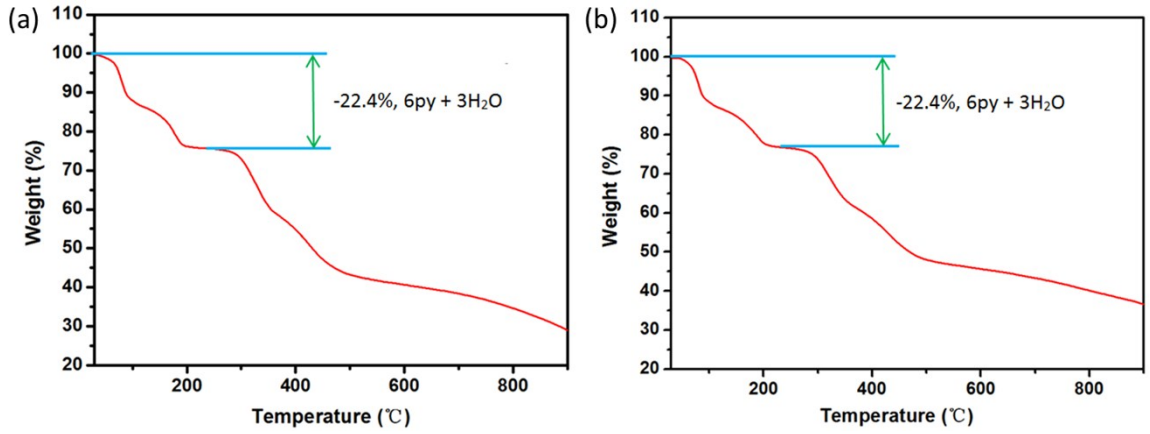

Figure S1. Thermogravimetric analysis of **1** (**a**) and **2** (**b**). The black solid lines show the loss of solvent molecules.

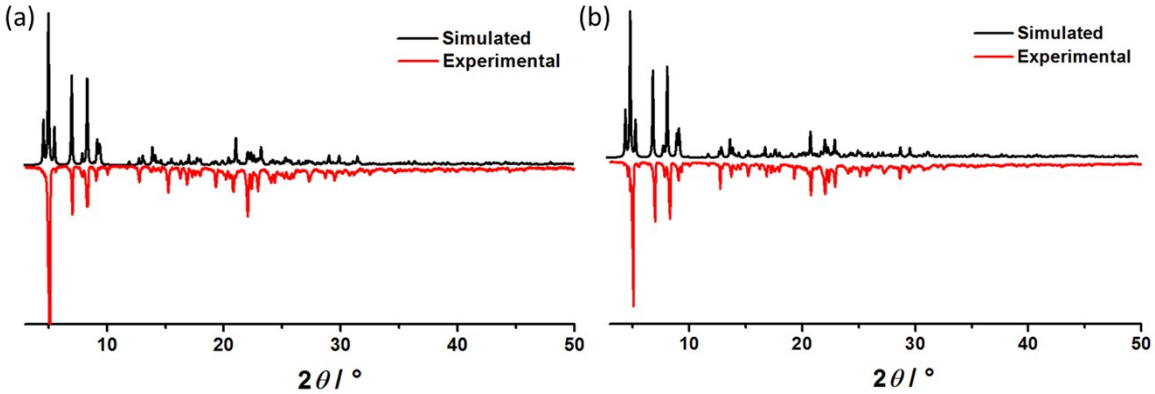

Fig. S2. Experimental and simulated powder X-ray diffraction (PXRD) for **1** (**a**) and **2** (**b**).

Table S1. Selected bond lengths [Å] and angles [°] for **1**-**3**.

1		**2**		**3**	
Eu1-O1	2.468(3)	Lu1-O1	2.422(3)	Y1-O1	2.440(3)
Eu1-O3	2.421(3)	Lu1-O3	2.376(3)	Y1-O3	2.399(3)
Eu1-O5	2.420(3)	Lu1-O5	2.362(3)	Y1-O5	2.390(3)
Eu1-O7	2.427(3)	Lu1-O7	2.367(3)	Y1-O7	2.392(2)
Eu1-O9	2.411(3)	Lu1-O9	2.363(3)	Y1-O9	2.381(3)
Eu1-O11	2.242(4)	Lu1-O11	2.151(3)	Y1-O11	2.195(3)
Eu1-O13	2.253(4)	Lu1-O13	2.159(3)	Y1-O13	2.197(3)
O1-Eu1-O3	70.71(12)	O1-Lu1-O3	70.75(9)	O1-Y1-O3	70.82(9)
O3-Eu1-O5	73.37(11)	O3-Lu1-O5	73.21(9)	O3-Y1-O5	73.30(9)
O5-Eu1-O7	71.86(11)	O5-Lu1-O7	71.90(9)	O5-Y1-O7	71.76(9)
O7-Eu1-O9	72.00(11)	O7-Lu1-O9	72.41(9)	O7-Y1-O9	72.27(9)
O9-Eu1-O1	72.16(11)	O9-Lu1-O1	71.90(9)	O9-Y1-O1	71.97(9)
O11-Eu1-O13	177.09(15)	O11-Lu1-O13	177.63(12)	O11-Y1-O13	177.50(11)

Table S2. Continuous shape measures calculations (CShM) for rare-earth ions in **1**-**3**.

Complex	HP-7 (D_{7h})	HPY-7 (C_{6v})	PBPY-7 (D_{5h})	COC-7 (C_{3v})	CTPR-7 (C_{2v})	JPBPY-7 (D_{5h})	JETPY-7 (C_{3v})
Eu in **1**	33.325	24.464	0.200	7.766	5.958	2.513	23.847
Lu in **2**	33.316	24.483	0.268	7.754	5.964	2.249	23.819
Y in **3**	33.291	24.547	0.232	7.838	6.009	2.361	23.879

*HP-7 = Heptagon; HPY-7 = Hexagonal pyramid; PBPY-7 = Pentagonal bipyramid; COC-7 = Capped octahedron; CTPR-7 =Capped trigonal prism; JPBPY-7 = Johnson pentagonal bipyramid J13; JETPY-7 = Johnson elongated triangular pyramid J7.

Table S3. Continuous Shape Measures (CShM) calculations for Cu(II) ions in **1-3**.

Complex	PP-5 (D_{5h})	vOC-5 (C_{4v})	TBPY-5 (D_{3h})	SPY-5 (C_{4v})	JTBPY-5 (D_{3h})
Cu1 in **1**	26.112	2.176	5.346	1.367	8.861
Cu2 in **1**	23.794	2.445	6.058	1.760	8.449
Cu3 in **1**	28.402	1.942	4.328	0.916	6.877
Cu4 in **1**	26.456	2.039	5.414	1.248	8.917
Cu5 in **1**	26.219	1.804	6.031	1.308	8.284
Cu1 in **2**	25.692	2.257	5.433	1.361	9.075
Cu2 in **2**	23.931	2.512	6.025	1.778	8.395
Cu3 in **2**	28.592	2.070	4.221	0.845	6.732
Cu4 in **2**	26.396	2.054	5.397	1.207	8.995
Cu5 in **2**	26.085	1.830	5.934	1.301	8.075
Cu1 in **3**	25.662	2.267	5.402	1.389	9.010
Cu2 in **3**	24.420	2.334	5.883	1.631	8.260
Cu3 in **3**	28.688	1.992	4.211	0.856	6.753
Cu4 in **3**	26.421	2.079	5.362	1.232	8.954
Cu5 in **3**	26.051	1.834	5.903	1.302	8.130

*PP-5 = Pentagon; vOC-5 = Vacant octahedron; TBPY-5 = Trigonal bipyramid; SPY-5 = Spherical square pyramid; JTBPY-5 = Johnson trigonal.

Table S4. Comparison of the average equatorial, axial Ln-O bonds and the CShM values of Ln ions.

Complexes	Ln-$O_{equatorial}$ bonds (Å)	Ln-O_{axial} bonds (Å)	O_{axial}-Ln-O_{axial} angle (°)	PBPY-7 (D_{5h})
{$EuCu_5$} (**1**)	2.429	2.248	177.09	0.200
{$LuCu_5$} (**2**)	2.378	2.155	177.63	0.268
{YCu_5} (**3**)	2.400	2.196	177.50	0.232
{$DyCu_5$} (**4**)	2.413	2.200	177.31	0.244

S2. Magnetic Characterization

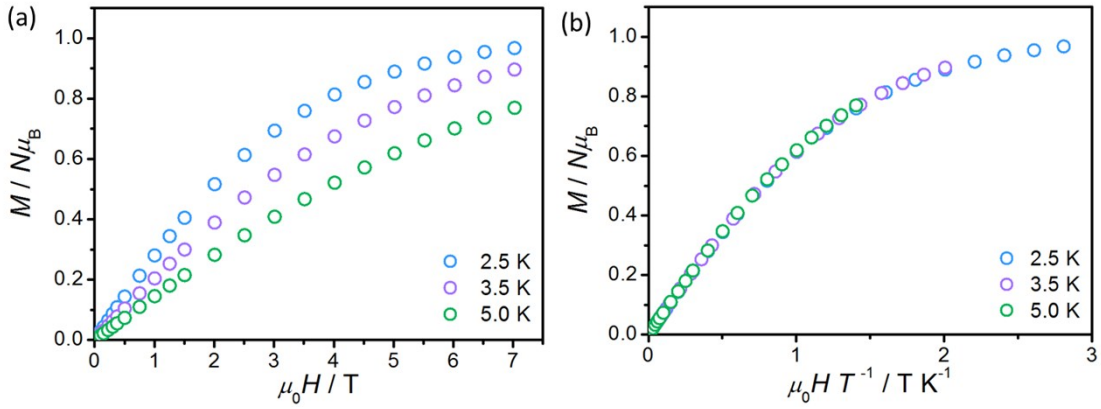

Fig. S3. Variable-field magnetization data (**a**) and the plot of *M vs*. HT^{-1} at different temperatures (**b**) for **2**.

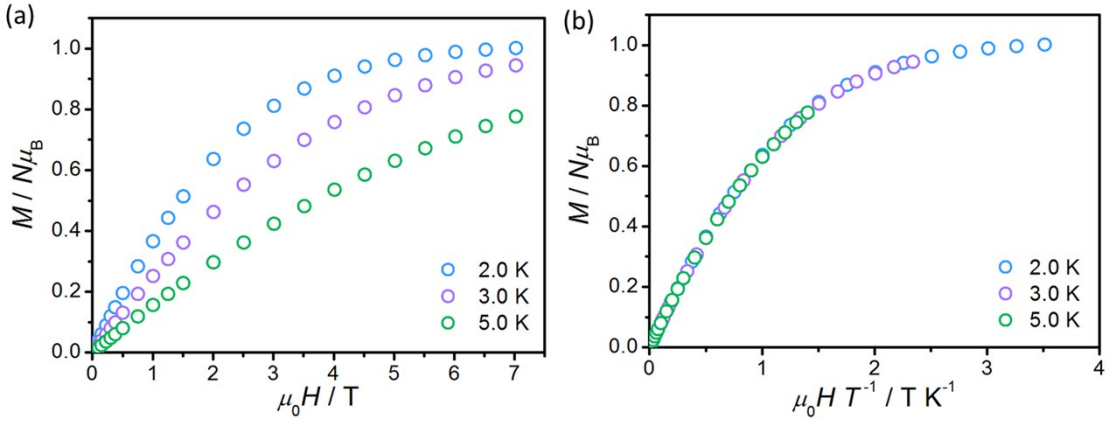

Fig. S4. Variable-field magnetization data (**a**) and the plot of *M vs*. HT^{-1} at different temperatures (**b**) for **3**.

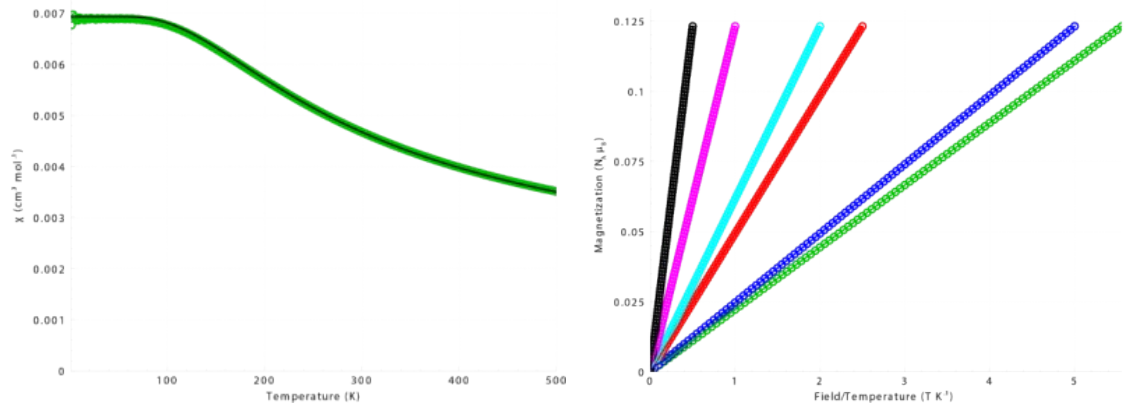

Fig. S5. Magnetic susceptibility and reduced magnetisation of the Eu^{III} ion in **1** calculated by CASSCF-SO (coloured circles) and with Equation 1 (solid lines).

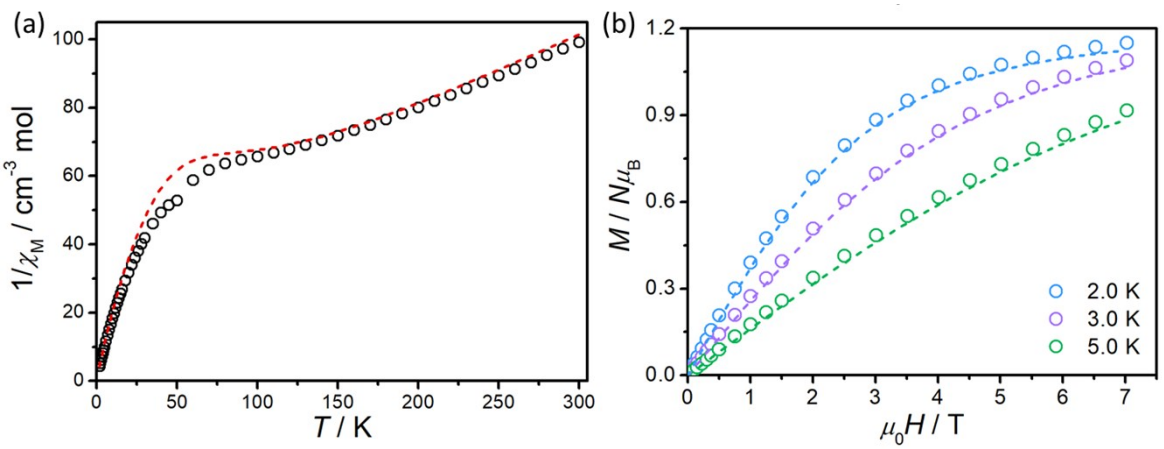

Fig. S6. Inverse magnetic susceptibility (a) and magnetisation (b) of {$EuCu_5$} (coloured circles) and those calculated with Equation 1 for $J_{Eu-Cu} = 0$ (solid lines).

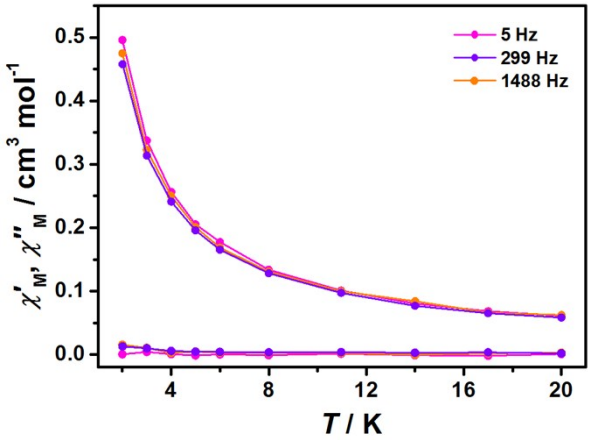

Fig. S7. Temperature-dependence of the in-phase (χ'_M) and out-of-phase AC susceptibilities (χ''_M) for **1** under 0 Oe DC field. The solid lines are guides for the eyes.

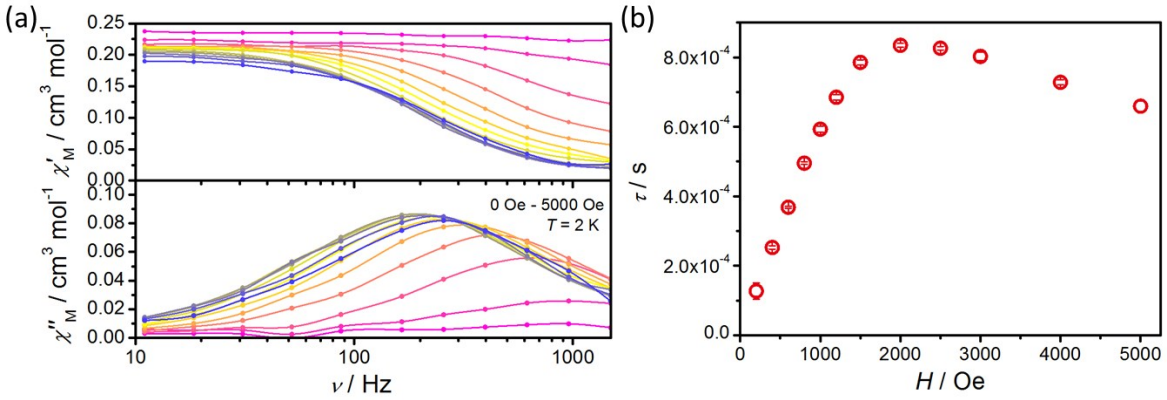

Fig. S8. (**a**) Frequency-dependence of the in-phase (χ'_M) and out-of-phase AC susceptibilities (χ''_M) at 2 K under different applied fields for **1**. The solid lines are guides for the eyes. (**b**) The field-dependent relaxation time for **1** at 2 K.

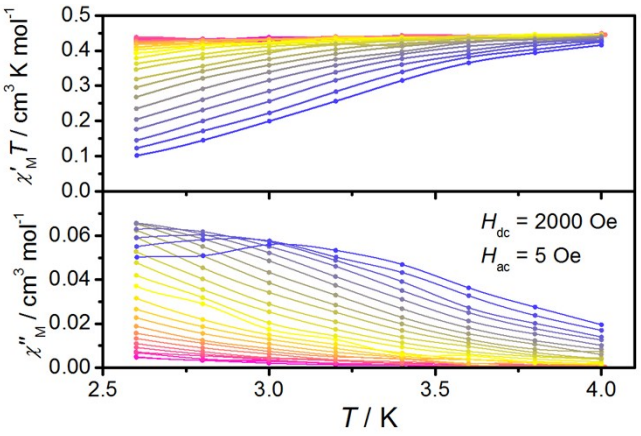

Fig. S9. Temperature-dependence of the in-phase (χ'_M) and out-of-phase AC susceptibilities (χ''_M) for **1** at 2 K under 2000 Oe DC field with the frequency of 1-1488 Hz. The solid lines are guides for the eyes.

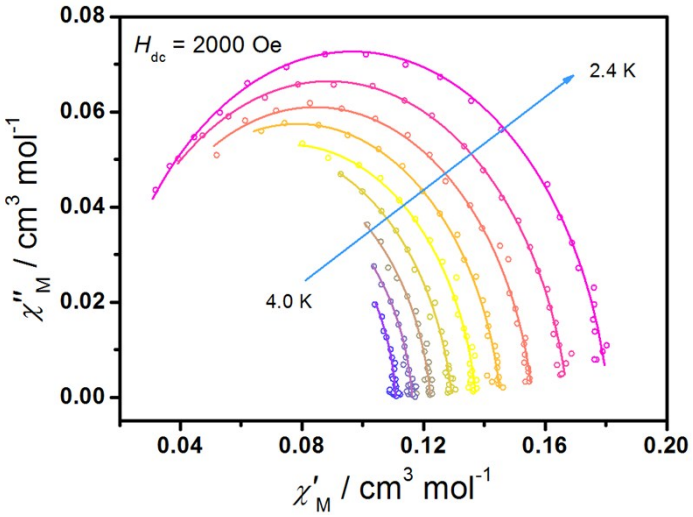

Fig. S10. Cole-Cole plots for the ac susceptibilities under 2000 Oe dc field for **1**. The solid lines are the best fit for the generalized Debye model.

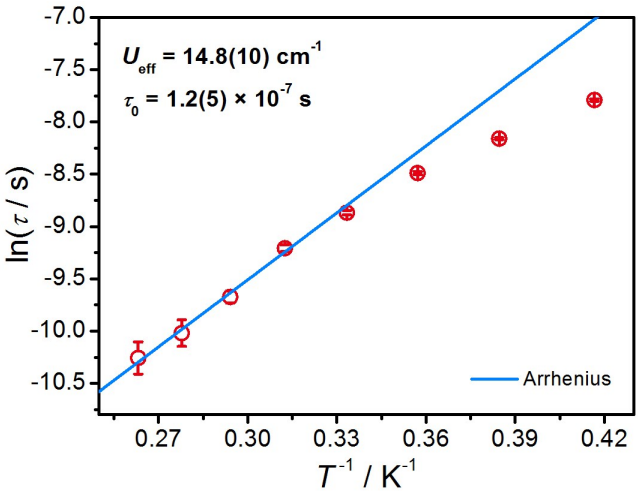

Fig. S11. The frequency-dependence of relaxation times for **1** under a 2000 Oe dc field. Blue lines are the fit of Arrhenius law.

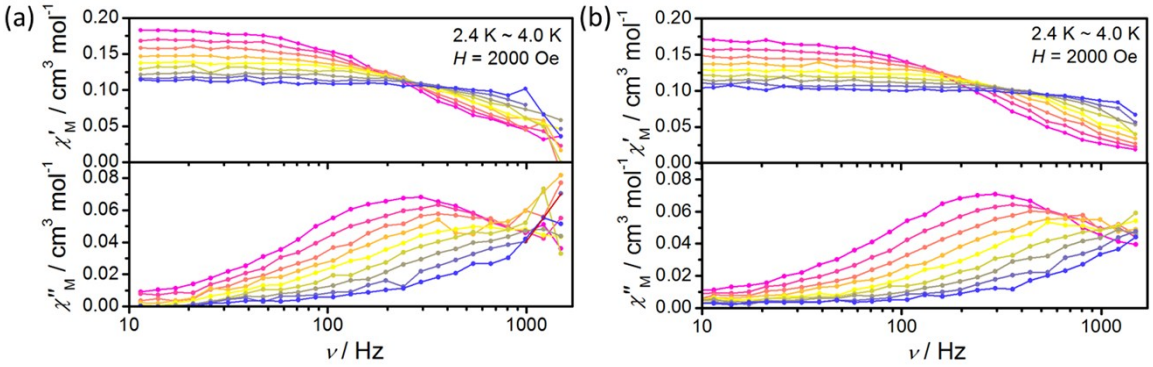

Fig. S12. The frequency-dependent of χ_M' and χ_M'' components of AC susceptibililties for **2** (**a**) and **3** (**b**) at 2000 Oe dc field.

S3. Theoretical Calculations

CASSCF-SO calculation

To obtain the electronic structure of the central Eu^{III} ion, an appropriate Hamiltonian to describe the Eu^{III} ion expressed in the $|L = 3, S = 3, m_L, m_S\rangle$ basis is:

$$\hat{H}_{Eu(III)} = \sum_{k\,=\,2,4,6} H_k^q \hat{O}_{kEu}^q + \sum_{j\,=\,1} \lambda_j \left(\vec{L}_{Eu} \cdot \vec{S}_{Eu}\right)^j + \mu_B \left(\vec{L}_{Eu} + 2\vec{S}_{Eu}\right) \cdot \vec{H}$$

(Equation S1)

where H_k^q are the crystal field (CF) parameters, $\hat{O}_{kEu}^q$ are the extended Stevens operators (which act on the orbital part of the wavefunction, i.e. these are constructed from $\hat{L}_{Eu}{}^2$, $\hat{L}_{Euz}$, $\hat{L}_{Eu+}$ and $\hat{L}_{Eu-}$ operators), λ_j are the SO coupling parameters (Karayianis, *J. Chem. Phys.*, 1970, **53**, 2460), $\vec{\hat{L}}_{Eu}$ is the orbital angular momentum operator, $\vec{\hat{S}}$ is the spin angular momentum operator, μ_B is the Bohr magneton and $\vec{H}$ is the magnetic field. Here, the deviation from the Landé interval rule is accounted for by phenomenological higher-order spin-orbit coupling terms first introduced by Karayianis (Karayianis, *J. Chem. Phys.*, 1970, **53**, 2460); in this way, the energy splittings of the *J* terms can be correctly accounted for without resorting to the entire $|4f^6\rangle$ microstate basis (where excited terms are so high in energy that they are not important for the magnetic properties).

Procedure to calculate the CF parameters

First we calculate the CF parameters for each of the *J* manifolds with SINGLE_ANISO (L. Ungur and L. F. Chibotaru, *Chem. Eur. J.*, 2017, **23**, 3708) and calculate the matrix representations of the CF Hamiltonians in each $|J, m_J\rangle$ basis. Then we calculate the matrix elements for each $\hat{O}_k^q$ operator in Equation S1 in the $|L = 3, S = 3, m_L, m_S\rangle$ basis, and transform the matrix representation of the $\hat{O}_k^q$

operators into the $|L = 3,S = 3,J,m_J\rangle$ basis using Clebsch-Gordan coefficients. We then fit the B_k^q CF parameters of Equation S1 in order to equate the sub-blocks of $\sum_{k = 2,4,6} B_k^q \hat{O}_k^q$ corresponding to specific *J* with the SINGLE_ANISO CF Hamiltonians in each $|J,m_J\rangle$ basis; this is particularly aided by the fact that only the CF operators with *k* = 2 have matrix elements in the *J* = 1 sub-block, only those with *k* = 2 or *k* = 4 have matrix elements in the *J* = 2 sub-block; the *k* = 6 terms can then be found by fitting the *J* = 3 sub-block. Then we fit the SO parameters to the barrycentres of the *J* manifolds, and finally fit the B_k^q parameters to the 49 SO energy levels and powder magnetisation and magnetic susceptibility data all from CASSCF-SO calculations (Table S5 and Figure S5).

Table S5. Hamiltonian parameters for Eu^{III}

Parameter	Value (cm^{-1})	Parameter	Value (cm^{-1})
B_2^{-2}	-0.8146	B_6^{-6}	-7.083
B_2^{-1}	-8.326	B_6^{-5}	-22.77
B_2^0	569.3	B_6^{-4}	-30.66
B_2^1	-28.14	B_6^{-3}	11.56
B_2^2	-22.19	B_6^{-2}	-9.049
B_4^{-4}	-27.66	B_6^{-1}	-3.067
B_4^{-3}	-1.295	B_6^0	24.49
B_4^{-2}	-8.621	B_6^1	-5.796
B_4^{-1}	36.93	B_6^2	13.54
B_4^0	128.3	B_6^3	-49.58
B_4^1	90.95	B_6^4	14.86
B_4^2	26.18	B_6^5	-2.612
B_4^3	-2.506	B_6^6	-3.486
B_4^4	-6.54	λ_1	233.5
		λ_2	-1.954
		λ_3	0.3901
		λ_4	-0.0002073
		λ_5	-0.003532
		λ_6	-0.0002068

Table S6. Lowest lying states for **1**, modelled with Equation 1 and $J_{Eu-Cu} = +1$ cm^{-1}

Energy (cm^{-1})
0.0
0.0
50.6
50.6
142.9
142.9
156.1

156.1
156.3
156.3